Harnessing cavity dissipation for enhanced sound absorption in Helmholtz resonance metamaterials

Electronic Supplementary Information

Xinwei Li,[a] Xiang Yu,[b] Jun Wei Chua,[a] and Wei Zhai*,[a]

[a]Department of Mechanical Engineering, National University of Singapore, 117575, Singapore.

[b]Department of Mechanical Engineering, The Hong Kong Polytechnic University, 999077, Hong Kong SAR.

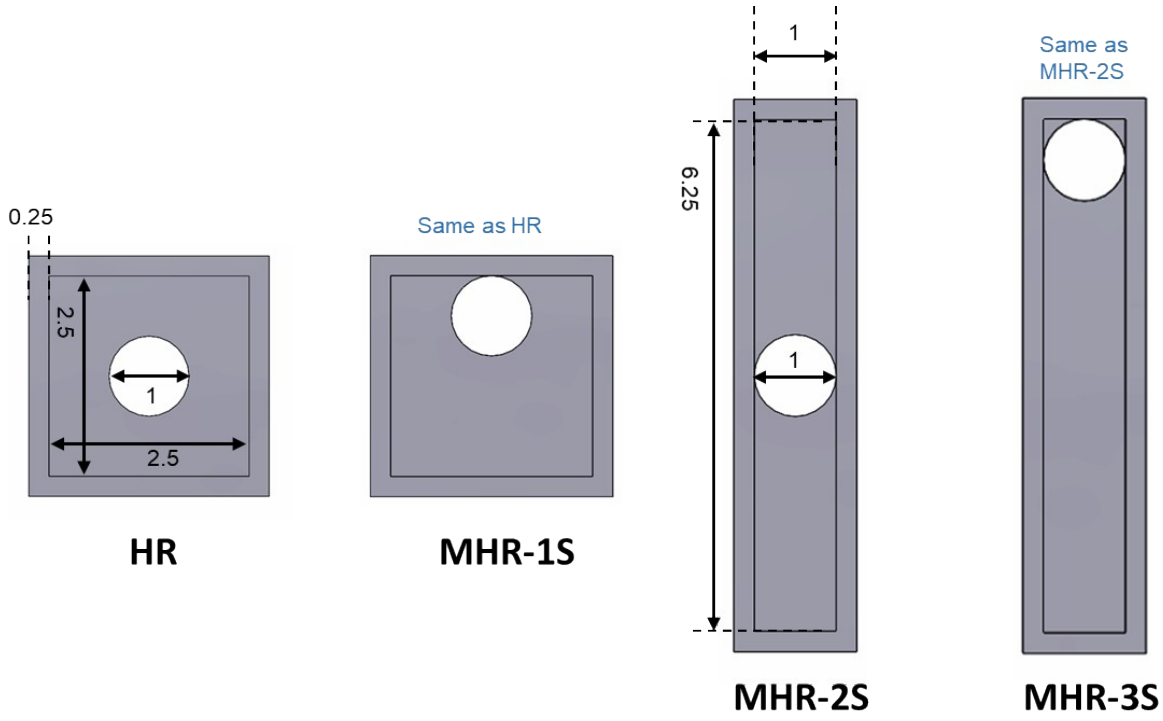

Fig. S1: The dimensions of HR and the modified MHRs as observed from the top view. Units are in millimetres.

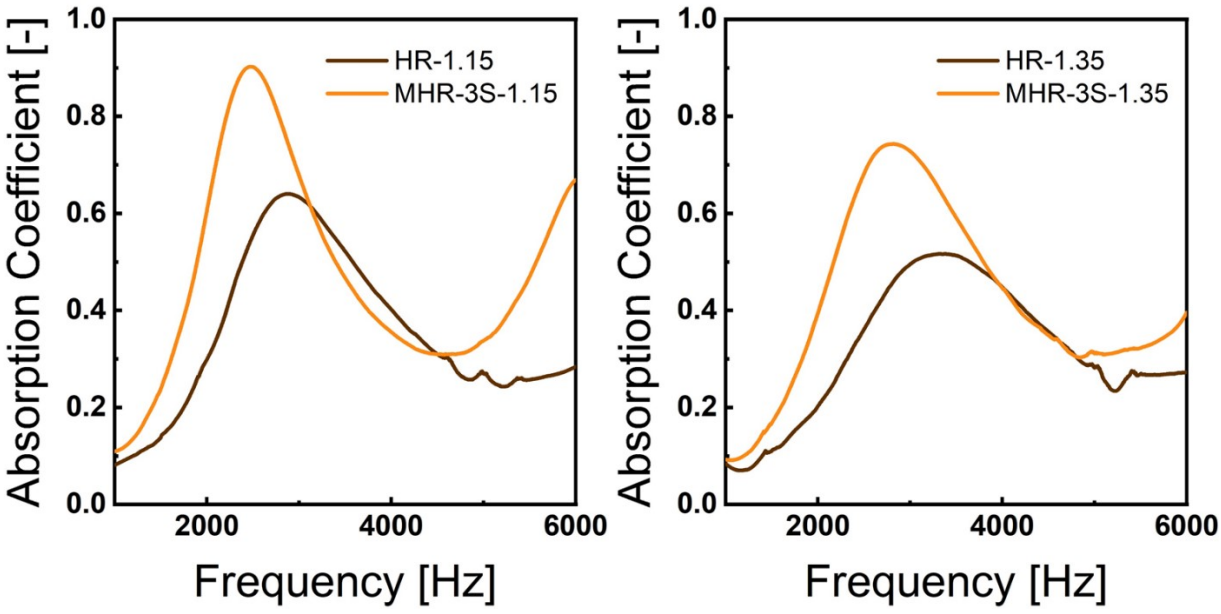

Fig. S2: Sound absorption coefficient curves of the HR and MHR-3S with pore diameters of 1.15 mm and 1.35 mm to supplement the trend presented in Fig. 2D.

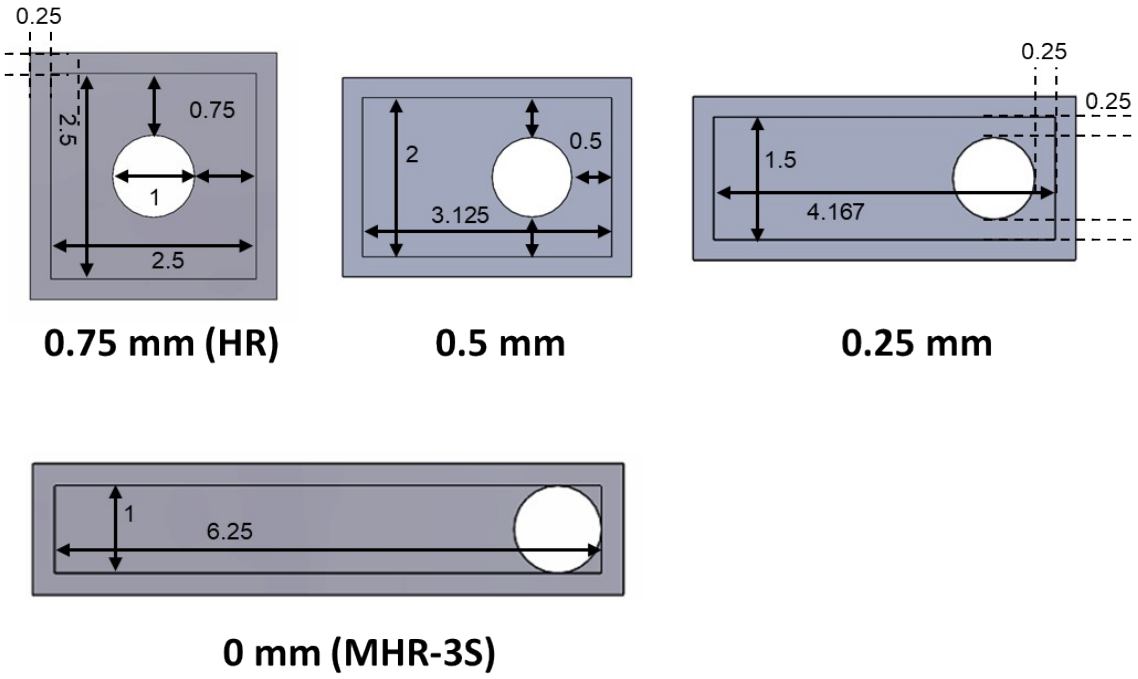

Fig. S3: The dimensions of the HR/MHR with varying pore and cavity wall separation distances. The cell wall thickness and the pore diameters are kept at 0.25 mm and 1 mm, respectively, for all of the cases. Units are in millimetres.

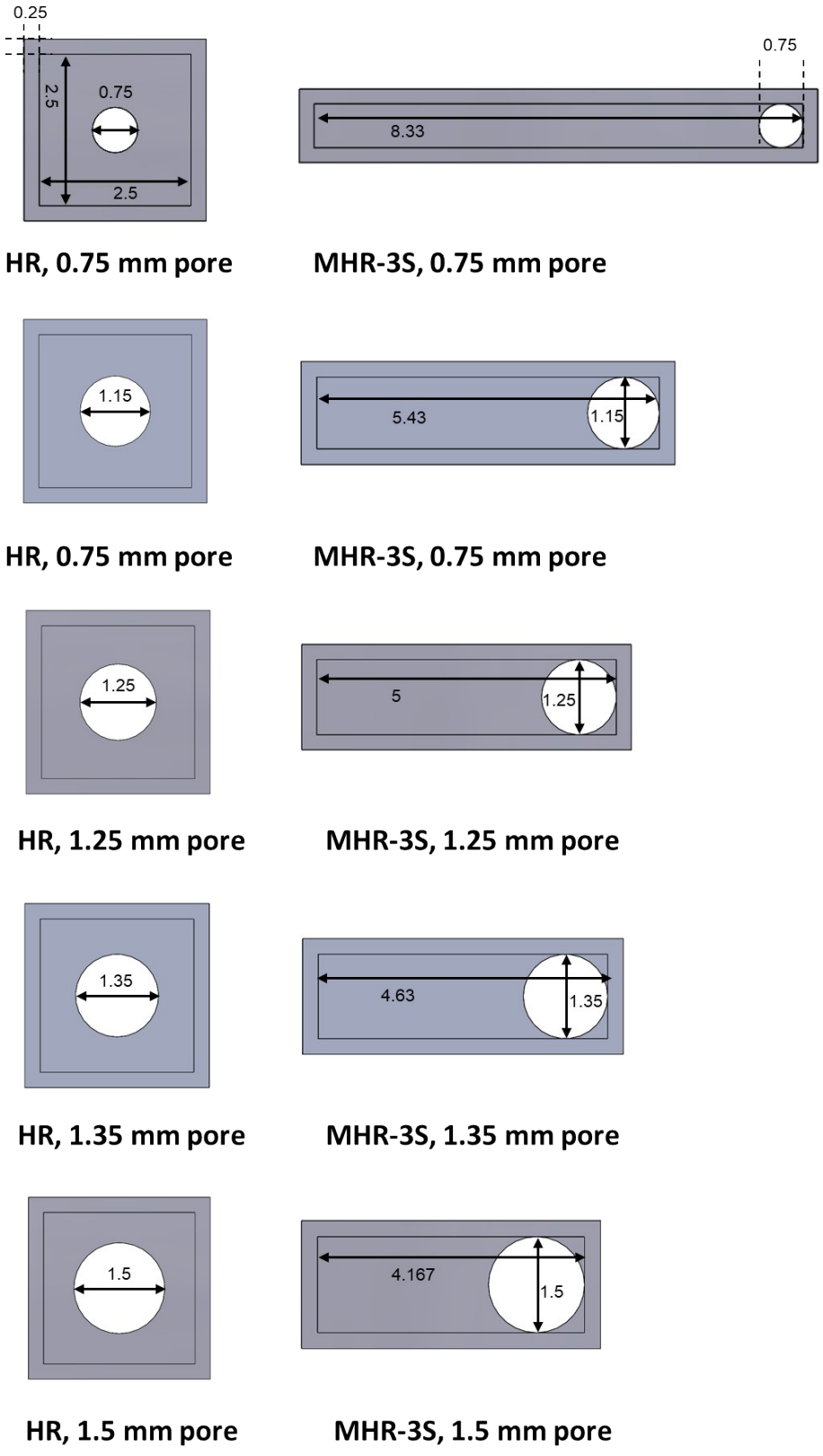

Fig. S4: The dimensions of the HR and MHR-3S with varying pore diameters. The cell wall thickness is kept at 0.25 mm for all of the cases. Units are in millimetres.

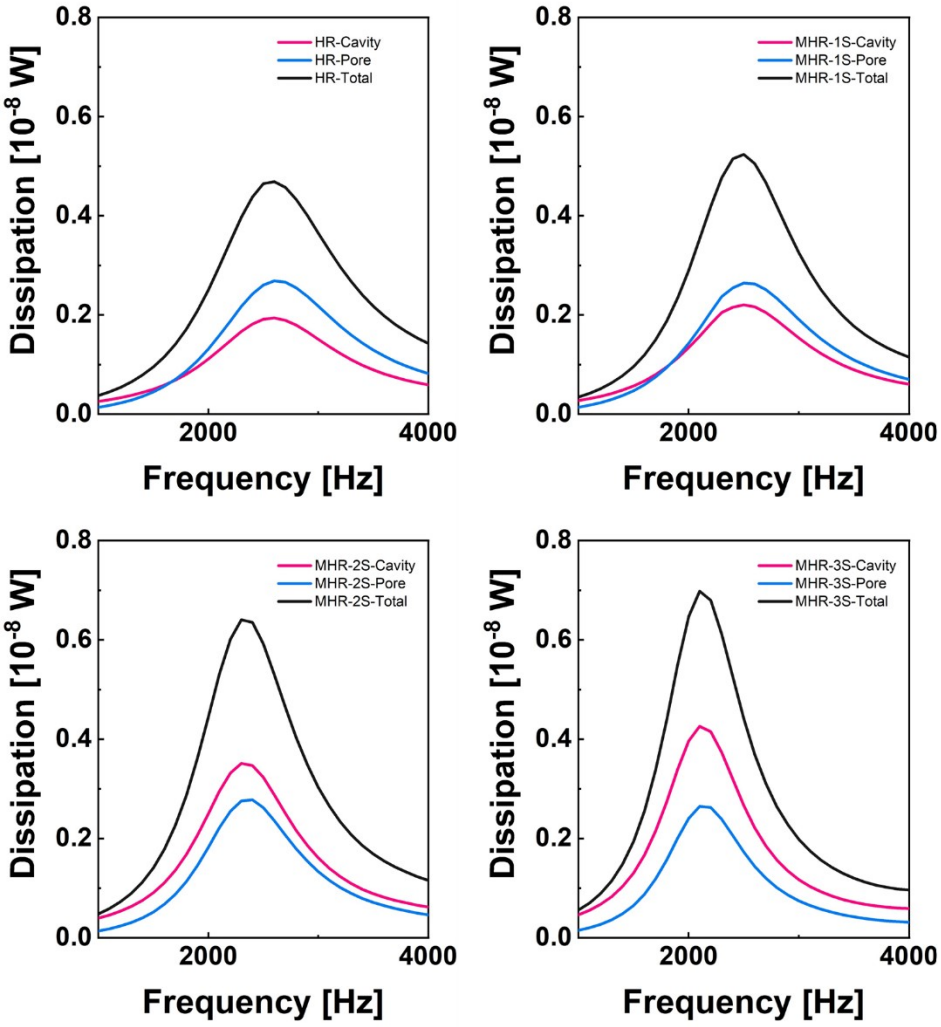

Fig. S5: The thermoviscous dissipation curves for the pores, cavities, and the total amount, in a single unit column of the HR and MHRs. The maximum values of the curves here are used to derive the overall dissipation plot shown in Fig. 3E.

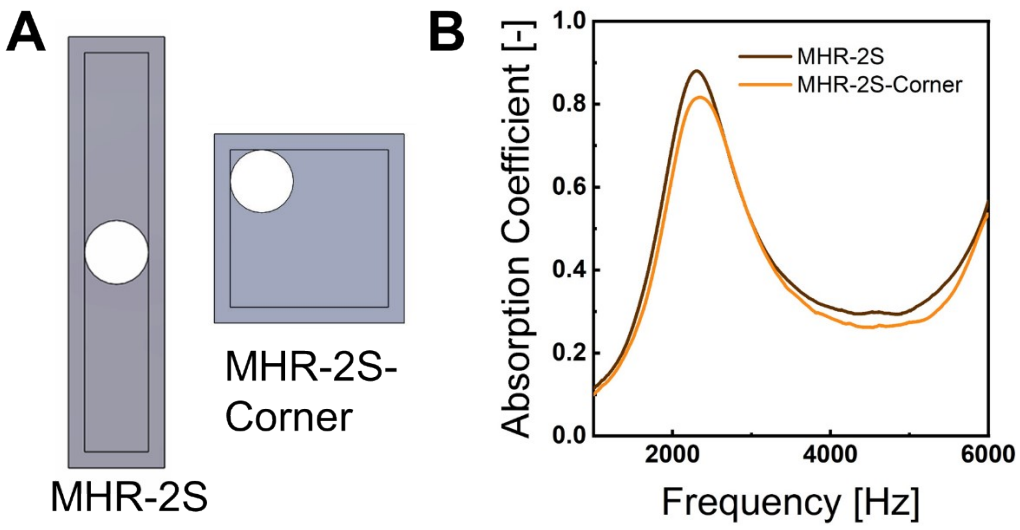

Fig. S6: (A) Illustration of MHR-2S and MHR-2S-Corner. MHR-2S-Corner has the exact same dimensions as that of an HR, with the only difference being the placement of the pore. (B) Sound absorption coefficient curves of the MHR-2S and MHR-2S-Corner, revealing the better absorption in MHR-2S.

Table S1: The explicit end correction expressions for HR and MHRs.

Increasing number of sides	**Expression**
ε	$\varepsilon = 7.9 + 1.9d + 0.5d^2$
δ	$\delta = 1.05 + 0.098d + 0.0625d^2$
Varying pore sizes	**Expression**
ε, HR	8
δ, HR	$\delta = 1.35 - 0.4d$
ε, MHR-3S	$\varepsilon = 171 - 668d + 1002d^2 - 621d^3 + 135d^4$
δ, MHR-3S	$\delta = 3.5 - 1.6d$

It should be noted that the trends observed for structures with an increasing number of sides are primarily for mathematical illustration rather than physical purposes. Structures with non-integer numbers of sides cannot be clearly defined.

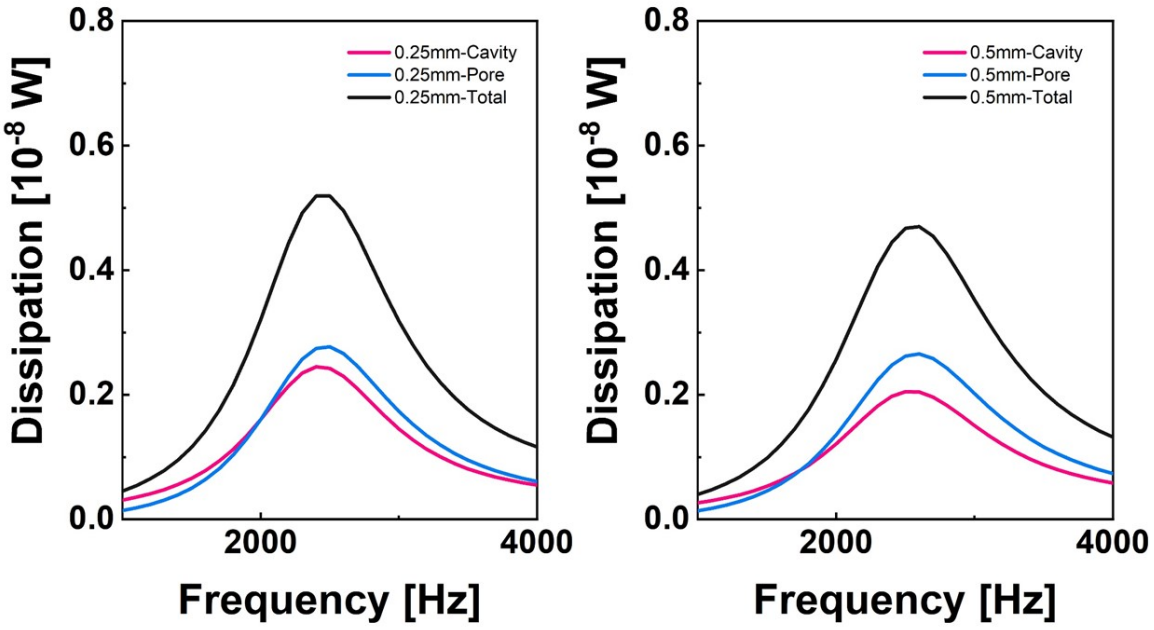

Fig. S7: The thermoviscous dissipation curves for the pores, cavities, and the total amount, in a single unit column of MHR-3S with 0.25 mm and 0.5 mm separation distance. Curves for the 0.75 mm (HR) and 0 mm (MHR-3S) cases can be found in Fig. S5. The maximum values of the curves here are used to derive the overall dissipation plot shown in Fig. 4B.

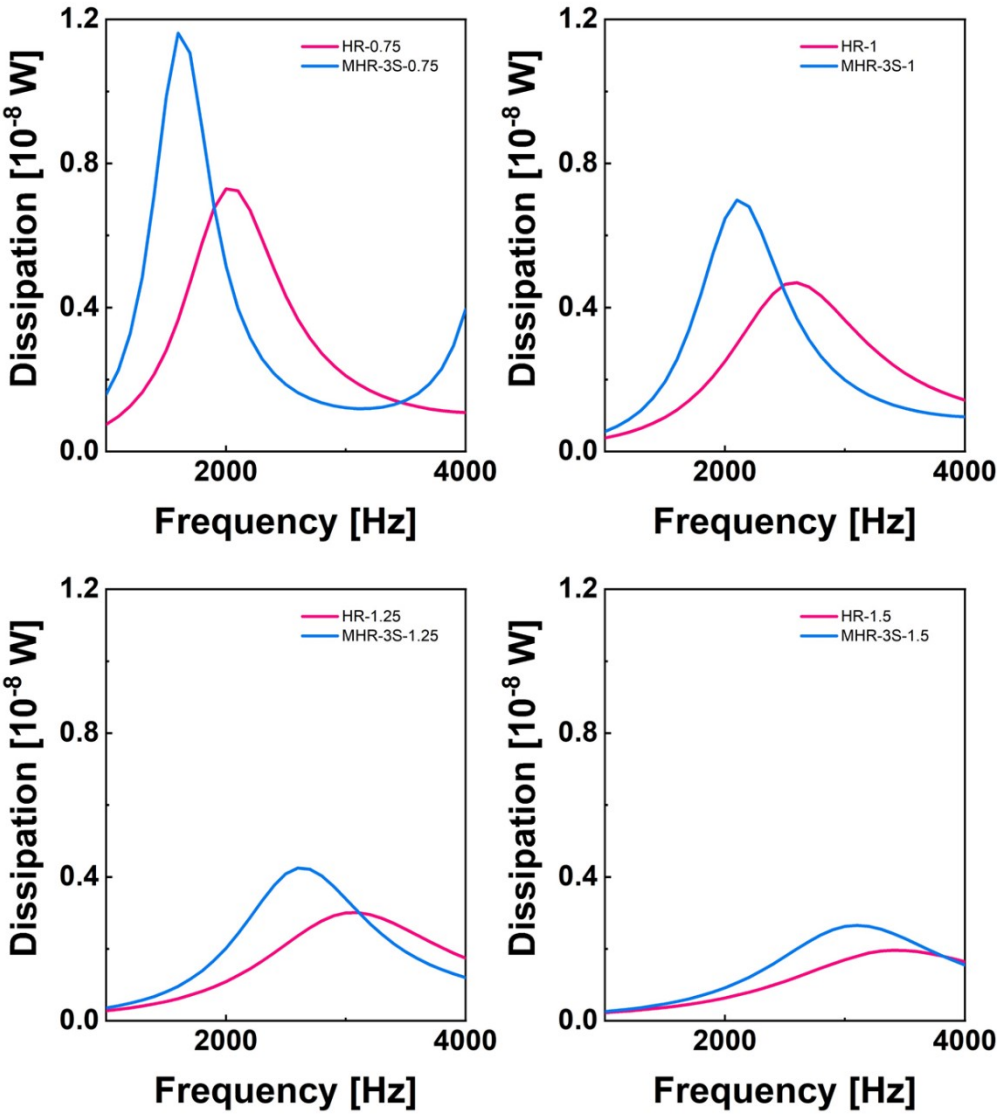

Fig. S8: The thermoviscous dissipation curves of a single unit column of HR and MHR-3S with varying pore diameters. The maximum values of the curves here are used to derive the overall dissipation plot shown in Fig. 4D.

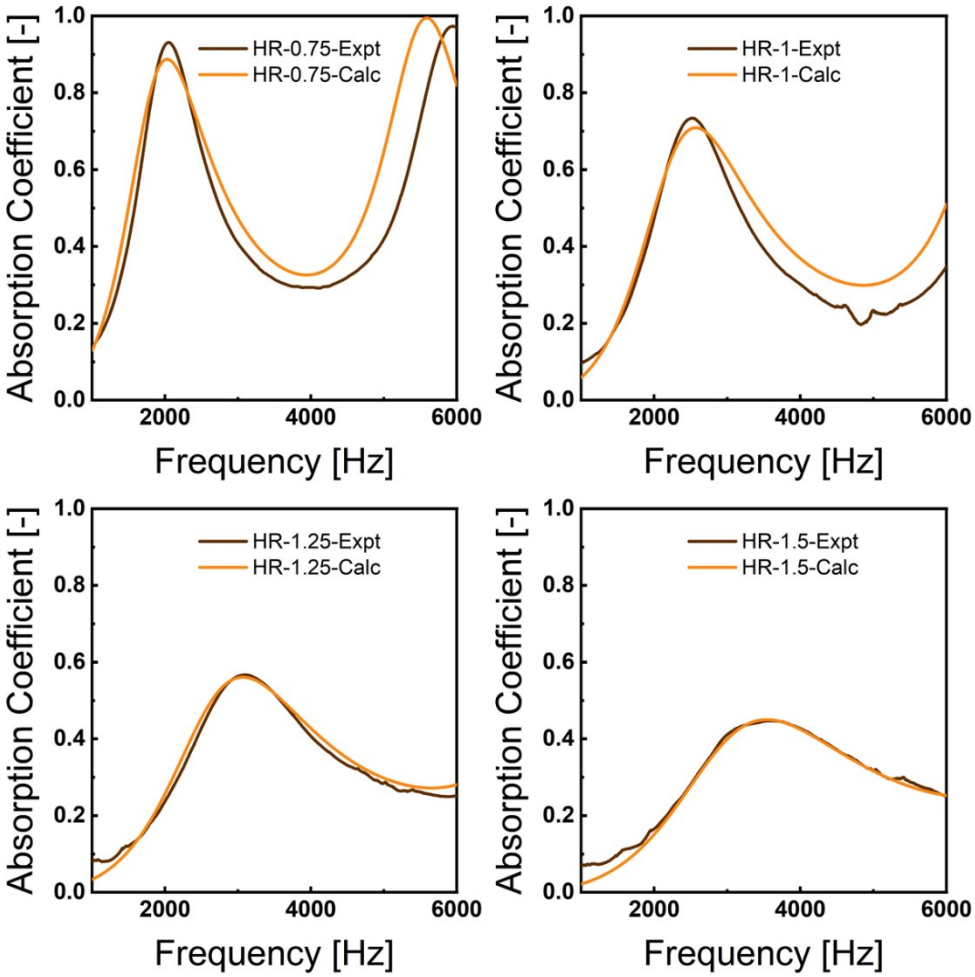

Fig. S9: Correlation between the experimentally-measured (Expt) and analytically-calculated (Calc) sound absorption coefficient curves of the HR samples with pore diameters of 0.75, 1, 1.25, and 1.5 mm.

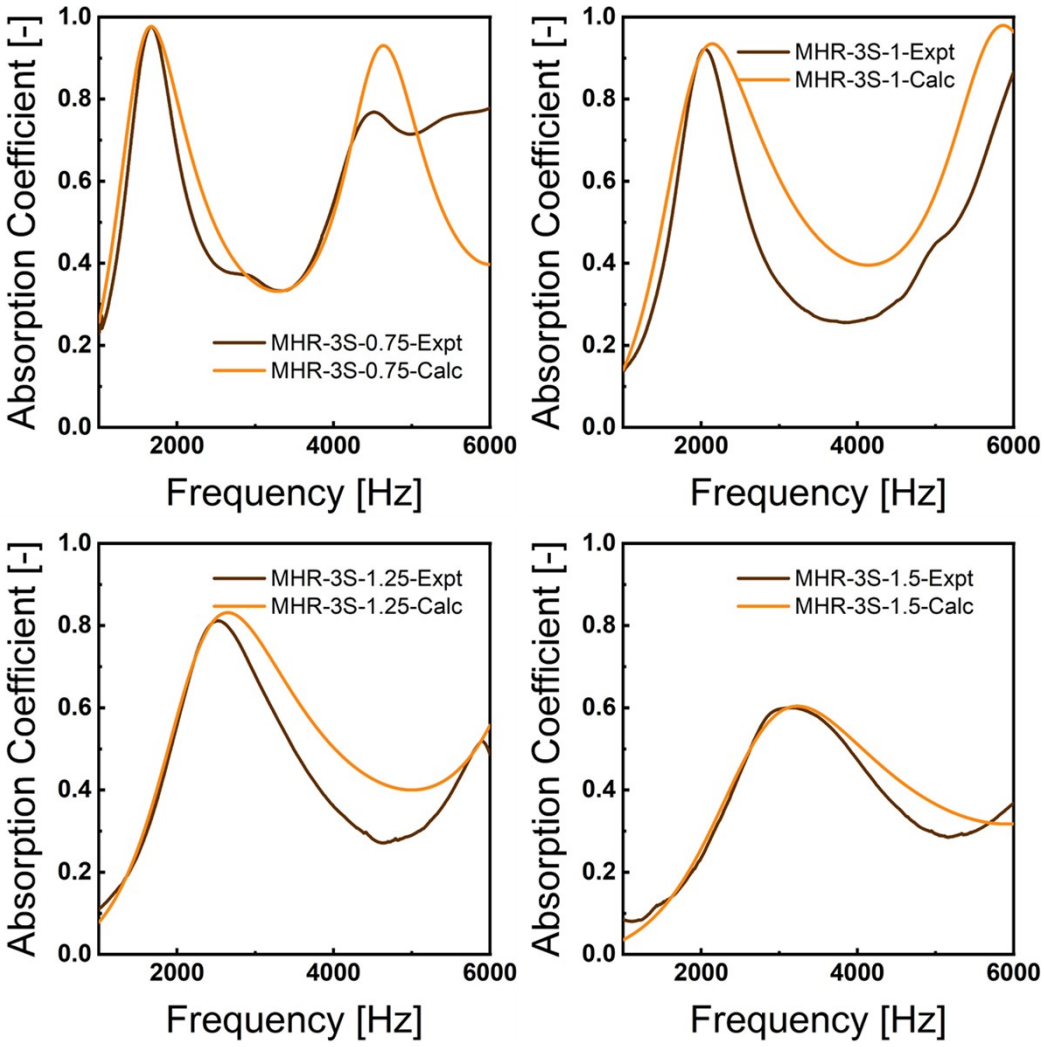

Fig. S10: Correlation between the experimentally-measured (Expt) and analytically-calculated (Calc) sound absorption coefficient curves of the MHR-3S samples with pore diameters of 0.75, 1, 1.25, and 1.5 mm.

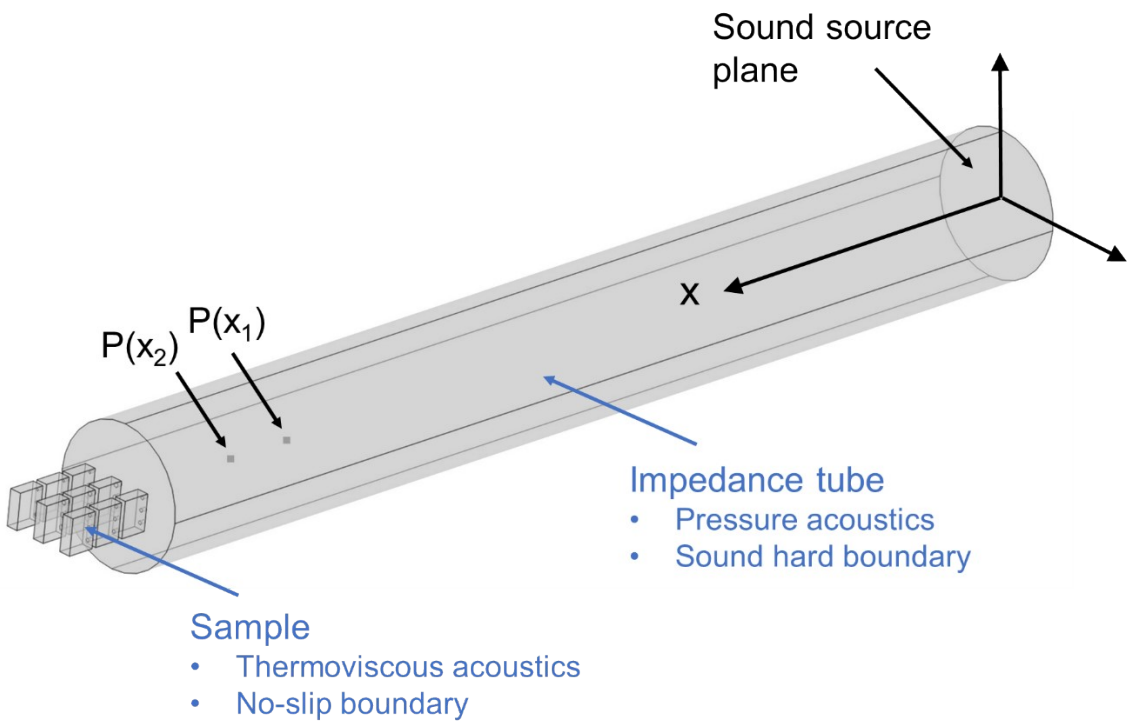

Fig. S11: The setup and details of the COMSOL FEM model used to analyze the thermoviscous dissipation.

The COMSOL Multiphysics finite element modelling (FEM) model is modelled after the configuration of an impedance tube (**Fig. S11**) with transfer function applied in accordance with ASTM E1050-19 standards. In contrast to the physical model, the FEM model used the air phase, which was subjected to appropriate boundary conditions, as the medium. The microphones, $P(x_1)$ and $P(x_2)$, used for signal collection were then modelled using two points that record pressure changes. Specific dimensions, based on the impedance tube used, are as follows:

- Length of tube: 235
- Distance from sound source to $P(x_1)$: 190
- Separation distance of $P(x_1)$ and $P(x_2)$: 15

To model the acoustic properties of the impedance tube and the samples (HR and MHR), the pressure acoustics and thermoviscous acoustics modules were applied, respectively. The Pressure Acoustics module was used to generate propagating planar sound

waves and to record pressure data points. Owing to the large impedance mismatch between the steel tube and air, boundary of the air column in the impedance tube can be simply set as sound hard, where no outward sound propagation can take place. On the other hand, the Thermoviscous Acoustics module was employed to analyse the viscous and thermal boundary losses of the sound waves across the internal features of the samples. This module is based on the assumption of isentropic acoustics and a lossless system, where the principle of loss is attributed to the viscous and thermal boundary layers. The boundaries for the samples are set to no-slip, whereby the airflow has zero velocity relative to the (hypothetical) walls of the samples.

After establishing the model and its boundary conditions, we next proceed to define the equations, in accordance with ASTM E1050-19 standards, for the calculation of the sound absorption coefficients. The total sound pressure at any distance x from the sound source can be expressed as:

$$P(x) = Ae^{-ikx} + Be^{ikx} \#(1)$$

A and B are constants and their terms refer to the incoming sound (from sound source), and reflected sound, respectively. k refers to the wave vector given by $\frac{2\pi}{\lambda}$, where λ is the wavelength. The sound pressures at positions 1 and 2 are then expressed as:

$$P(x_1) = Ae^{-ikx_1} + Be^{ikx_1} \#(2)$$

$$P(x_2) = Ae^{-ikx_2} + Be^{ikx_2} \#(3)$$

x_1 and x_2 represent the separation of each microphone from the sound source, respectively. Following the sound pressure generation, the pressures $P(x_1)$ and $P(x_2)$ are then calculated based on point integration at the point. Following this, we define a transfer function, H, between points 1 and 2 as:

$$H = \frac{P(x_2)}{P(x_1)} \#(4)$$

$$H = \frac{Ae^{-ikx_2} + Be^{ikx_2}}{Ae^{-ikx_1} + Be^{ikx_1}} \#(5)$$

$R = \frac{B}{A}$ is the complex reflection coefficient:

$$R = \frac{e^{-ikx_2} - He^{-ikx_1}}{He^{ikx_1} - e^{-ikx_2}} \#(6)$$

With the value of H known, R is then solved through Equation (6). Finally, the absorption coefficient is calculated using the following transformation:

$$\alpha = 1 - |R|^2 \#(7)$$

The abovementioned equations were defined in COMSOL. The absorption coefficient curve can then be obtained via sweeping across the desired frequency range in the Frequency Domain Study. The resonant frequencies of each structure could then be identified and their respective dissipation colour maps shown in **Fig. 3,4** are then obtained by plotting the built-in "ta_diss_tot" function. The thermoviscous dissipation curves are obtained by volume integration of the relevant structures (pore, cavity, or the total unit), using "ta_diss_tot".

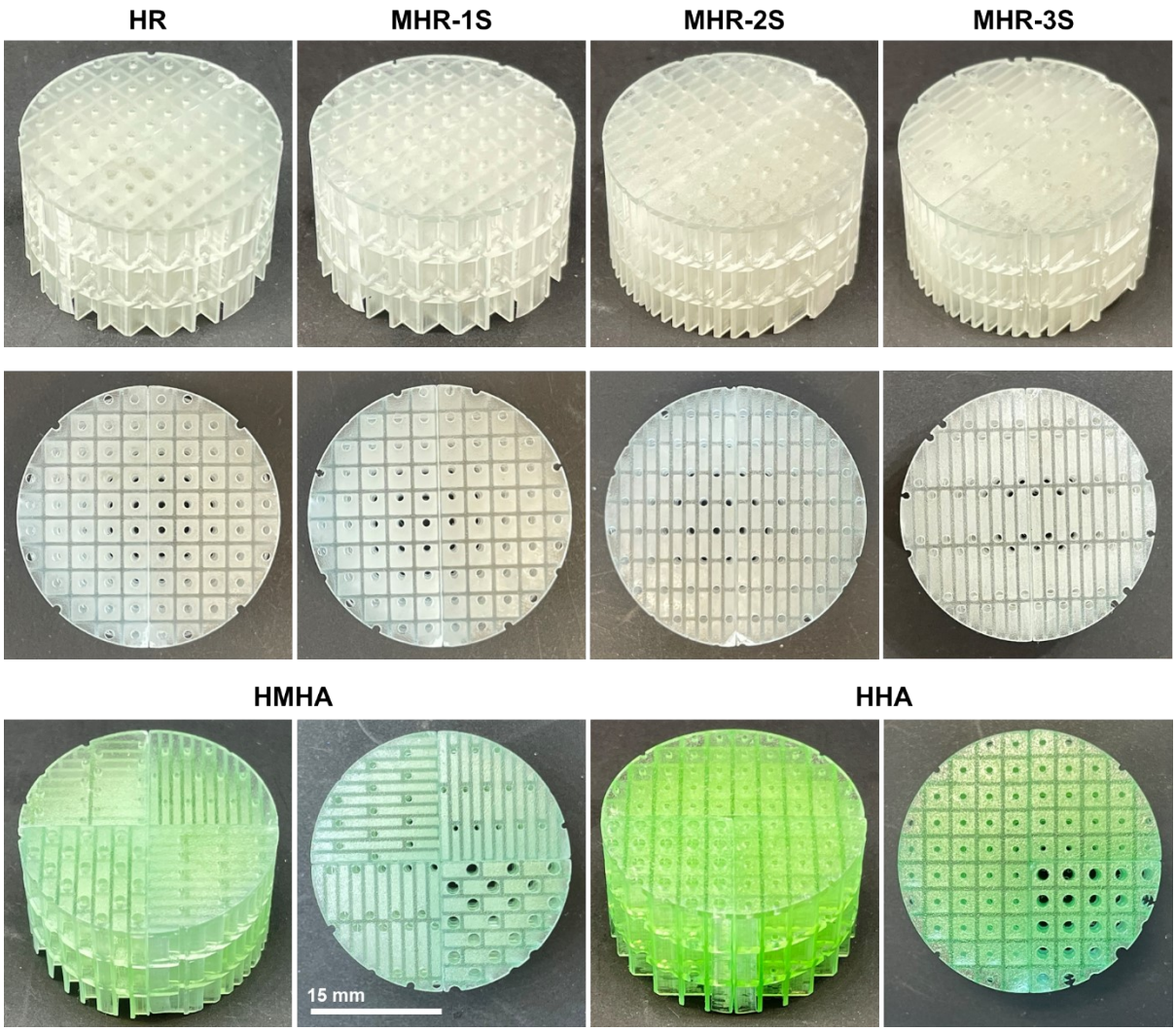

Fig. S12: Digital images of a few selected as-printed samples. The MHR-3S structures with varying separation distance and pore sizes are designed and 3D printed through the similar methodology. The height of all samples is 18 mm.